Probe Coherence Volume and the Interpretation of Scattering Experiments

N. Bernhoeft,[1,2] A. Hiess,[1] S. Langridge,[2,3,4] A. Stunault,[2] D. Wermeille,[2] C. Vettier,[2] G. H. Lander,[3] M. Huth,[5]
M. Jourdan,[5] and H. Adrian[5]
[1]*Institut Laue Langevin, BP 156, F-38042 Grenoble, France*
[2]*European Synchrotron Radiation Facility, BP 220, F-38043 Grenoble, France*
[3]*European Commission, JRC, Institute for Transuranium Elements, Postfach 2340, D-76125 Karlsruhe, Germany*
[4]*Rutherford Appleton Laboratory, ISIS Facility, Chilton, Didcot, Oxon OX11 OQX, United Kingdom*
[5]*Institut für Physik, Johannes-Gutenberg-Universität, D-55099 Mainz, Germany*
(Received 26 June 1998)

We discuss the importance of the probe coherence volume in the interpretation of diffraction experiments. The availability of highly monochromatic radiation, neutron or x-ray, calls into question the analysis of data by deconvolution at the level of intensities. When the probe coherence volume approaches that of microscopically ordered regions in the sample, new effects may be anticipated. For instance, under strong absorption the intensity dependence on the incident energy can be used to locate the source of the scattering below the sample surface. Two examples, based on experiments at an x-ray synchrotron source are discussed. [S0031-9007(98)07438-9]

PACS numbers: 61.10.Dp, 75.25.+z

Much of our microscopic understanding about a wide range of phase transitions derives from detailed scattering experiments. The proportionality of the differential scattering cross section to a two site correlation function was pointed out by van Hove, and is fundamental to the interpretation of such experiments [1]. The basic interactions are extensively discussed in the literature for both x-ray and neutron scattering [2] and rest on the assumption that the state function may be separated into two parts, that of the probe and that of the sample; i.e., the scattering process may be represented by a sufficiently weak interaction (cf. Born approximation). Further, the measured intensity is also separated into two parts being represented as the convolution of an intrinsic sample response and the resolution function of the spectrometer. When the partial beam coherence is high [3,4], this latter assumption may be called into question.

The incident beam, considered as a sum of elemental rays, may be said to present a significant degree of partial coherence when the typical coherence volume of a ray is similar in size to an elemental diffracting volume (e.g., mosaic block) in the sample. The ray coherence volume has a longitudinal dimension, parallel to the propagation direction, given by $\lambda/(\Delta\lambda/\lambda)$, where λ is the wavelength of the radiation and the wavelength spread is $\Delta\lambda$, and two, orthogonal, transverse dimensions which vary inversely with the source size [4]. While similar effects are anticipated for all scattering techniques, advances in providing highly collimated monochromatic beams have been especially rapid at synchrotron sources. The routine availability of x-ray beams with a probe coherence dimension substantial on the scale of 1 μm has stimulated the experimental background to the discussion. Indeed, using spatial filtering techniques, this coherence has already been exploited in the observation of *intensity* correlation (speckle) patterns by x rays [5]; however, this is not our concern. Rather we consider effects which may be present in conventional, high resolution, diffraction (*amplitude* correlation) experiments when using partially coherent illumination.

Diffraction profile analysis, before inclusion of the instrumental resolution, often rests on the joint (implicit) assumptions that, first, the effective ray coherence volume is always larger than the diffracting region (i.e., the ray coherence length only enters, indirectly, at the level of the intensity convolution with the resolution function). Second, that, when accounting for the effects of absorption, the beam penetration depth is, likewise, much greater than the size of the elemental diffracting volume, in order to justify calculations based on the summation of diffracted intensities. As an important example of the breakdown of these assumptions, we show that, when the absorption depth is similar to or smaller than the scale of the coherent diffracting volume, the beam attenuation must be taken into account at the level of the scattering *amplitude*. This negates, in such instances, the possibility to make data analysis by convolution at the level of intensities.

We discuss then, the novel situation in which partially coherent beams enter a highly absorbing medium, as may be the case when experiments are conducted at synchrotron sources with photons whose incident energies lie near absorption edges. Such experiments have become common in examining magnetic phenomena using x-ray resonant exchange scattering (xres), particularly in materials involving the rare earths and actinides, where the L and M absorption edges, respectively, occur at energies suitable for scattering experiments. We show below that, in this limit, calculations must take into account both the probe coherence length and absorption effects on the scattering amplitude, and further that the *incident photon energy* dependence of the scattering may convey information about the *spatial location below the sample surface*

0031-9007/98/81(16)/3419(4)$15.00

of the scattering centers. This latter point increases the analytical power of the xres technique for investigating magnetic phenomena.

We take, as an example, xres experiments at the M_4 absorption edge of uranium. In this case the inverse linear absorption coefficient $1/\mu \sim 2000$ Å, and one has to consider the change in amplitude of the probe wave function occurring within the diffracting volume. Empirically, wave function amplitudes are inaccessible, and one measures intensities, given by the modulus of the scattered amplitude squared. Focusing attention on the variation of reflected intensity with incident photon energy at a Bragg point, i.e., all scattering elements in phase, for a resonant process represented by a Lorentzian line shape [6], one has

$$I \propto \frac{\Gamma^2}{\Gamma^2 + (\Delta E - \hbar\omega)^2}\left[\frac{1 - e^{-\mu^* Na}}{1 - e^{-\mu^* a}}\right]^2,$$

where, for a beam incident at angle α and exiting at angle β, $\mu^* = (\mu/2)[1/\sin(\alpha) + 1/\sin(\beta)]$. The formula splits naturally into two parts, both dependent on the incident photon energy. In the first factor, Γ is the inverse lifetime of the scattering process ($\sim$2.2 eV at the uranium M_4 [7]), ΔE is the energy difference between the initial and intermediate states of the resonant process (3728 eV at the uranium M_4 edge), and $\hbar\omega$ is the incident photon energy. In the second part, we consider the coherent sum of N diffracting planes parallel to the surface with a the interplanar spacing. When few layers contribute to the coherent sum, $\mu Na \ll 1$, the role of absorption may be neglected over the elemental scattering volume, and the total absorption of an extended (semi-infinite) sample yields an intensity proportional to $1/\mu$ [8]. In the case $\mu Na \geq 1$, the incident energy dependence of the scattering gives significantly more information.

We demonstrate the role of beam coherence in the presence of strong absorption on diffraction profiles with a model calculation for the energy dependence of an antiferromagnetic reflection at the uranium M_4 edge. The calculations, for the (0 0 0.5) reflection in UPd_2Al_3, are given by the open circles in Fig. 1 and correspond to the first of the two experiments discussed below. The M_4 absorption coefficient used in the calculation has been taken from that measured in UO_2 films [7], and the energy width and pole position of the resonance are fixed likewise from a parametrization of the UO_2 absorption peak. The sole variable of calculation is then N. The results, for different N (i.e., number of diffracting layers), are shown in Fig. 1. The solid lines are best fits with a Lorentzian function. At the top, low N, the profile in energy is Lorentzian with a half width half maximum (HWHM) equal to that of the measured absorption curve, $\Gamma = 2.2$ eV. On increasing N a broadening is seen which develops (lower figure) into two distinct peaks, the high energy peak being less intense on account of the increased absorption above the edge. The substantial broadening (to HWHM $\sim$5 eV) and eventual splitting of the peak may be understood as arising from a reduction in the effective scattering volume at the resonant energy. This cautions that values of the resonant width (core-hole lifetime) in the literature, obtained from samples thick compared with their absorption depth, may need to be reconsidered depending on the absorption length of the material and the degree of coherence of the incident beam.

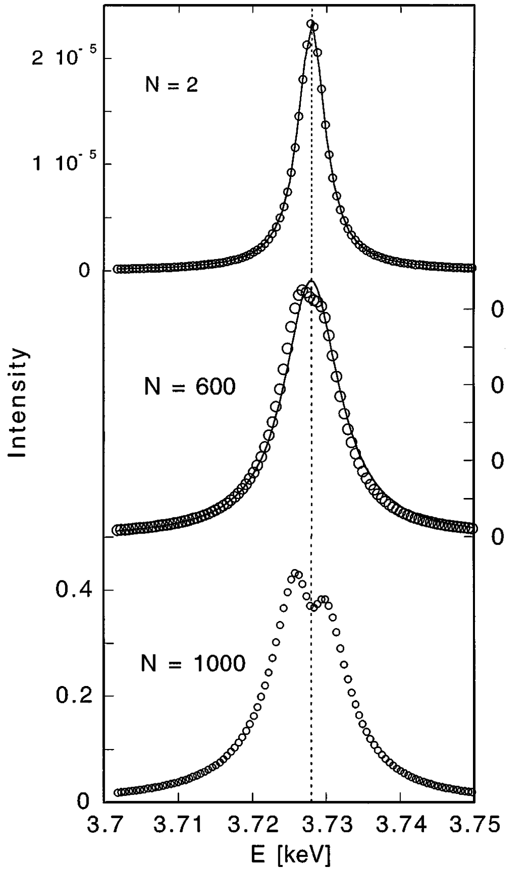

FIG. 1. Calculated energy profiles at the Bragg point as a function of incident photon energy near the M_4 uranium absorption edge (marked with dashed line at $E = 3.728$ keV). From top to bottom, 2, 600, and 1000 lattice planes are scattering. For less than $\sim$600 planes the profile remains Lorentzian, but continually broadens with increasing N.

We illustrate application of these ideas with results from two experiments performed on the ID20 beam line of the European Synchrotron Radiation Facility. ID20 views radiation from an undulator source with typical transverse coherence dimensions of 10 μm × 20 μm in the horizontal and vertical directions, respectively, combined with an incident energy bandpass of 10^{-4} giving a longitudinal probe coherence of 1 μm. The samples were thin films of hexagonal UPd_2Al_3 and a single crystal of UAs. The films were grown epitaxially on the (111) surface of $LaAlO_3$ by coevaporation of the elements [9] with their c axis perpendicular to the surface. The mosaic spread about the c axis is $\sim$1.2° to 0.3° for films of thickness 100 to 1600 Å. Our observation of the (0 0 0.5) and (0 0 1.5) antiferromagnetic peaks in all films shows that the antiferromagentic order is the same as in the bulk [10]; a simple doubling along the c axis, with the moments lying in the plane of the film. The energy profile for all reflections at $T = 4$ K is approximately Lorentzian. In Fig. 2 we plot the observed HWHM as a function of the optical path of the photon beam through the sample. The heavy dashed line is derived from the calculations outlined above with the assumptions that (i) the antiferromagnetic ordering permeates the *whole* film thickness (except in the case of the thinnest 100 Å film, where the observation of magnetic fringes enabled us to determine the magnetic thickness directly as being 75 Å); i.e., N is determined, and (ii) the resonant energy width and positions are given by the absorption peak parametrized in UO_2. The agreement between the calculation and experiment lends support to the suggested treatment. For contrast, we also plot, as a continuous line, the energy widths that are obtained by summation of diffracted intensities (linear theory using measured absorption curve of HWHM 2.2 eV) with a resonant energy width (3.54 eV) fixed to reproduce the observed bulk value. In addition to the poor agreement with the data from the thin films where absorption corrections ought to be minimal, it is not obvious to understand why, in this approach, the resonant width needs to be taken so much greater than the absorption width.

Interestingly, the energy profile at the (0 0 0.5) reflection in the 1600 Å film shows a *narrowing* (by 20%) near T_N (14 K). Calculation within the coherent approximation allows us to locate the depth below the surface of the source of the magnetic scattering. The energy profile is consistent with *only the top* 600 (±50) Å being magnetically ordered, the solid line in Fig. 3. In contrast, if the order had been nucleated at the base of the film, the profile would have exhibited a broadening together with a dip at the resonant energy, the dashed line Fig. 3. A study of the specular wave vector HWHM, at constant incident energy, reveals only the spatial correlation length and *not* the location of the diffracting volume. We deduce then that magnetic order is nucleated in the near surface of the sample and propagates into the bulk on lowering the temperature.

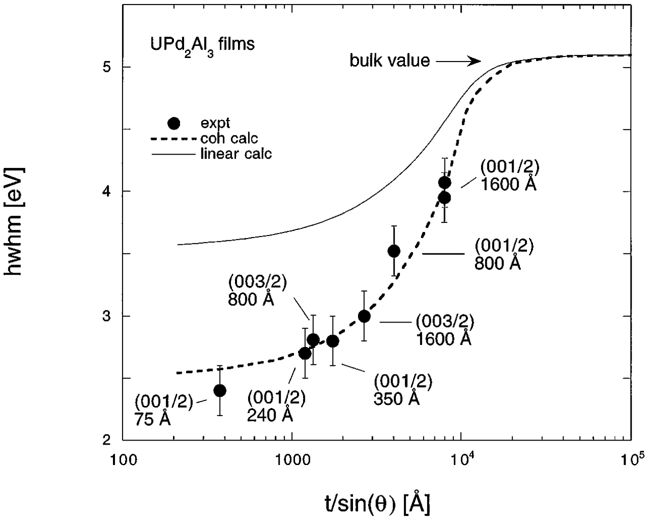

FIG. 2. Energy HWHM of the antiferromagnetic peaks (at $T = 4$ K) measured at the M_4 absorption edge as a function of optical path ($t =$ film thickness, and θ is the Bragg angle for a reflection) of the photon beam in the thin films of UPd_2Al_3. The heavy dashed curve is the numerical simulation in the coherent approximation as discussed in the text. The continuous line arises from a classical (incoherent) summation of intensities.

The second example concerns experiments performed on a thick crystal (approximately 1 mm) of UAs orientated with an (001) face in specular geometry. In Fig. 4(a) we show the wave vector profile at the resonant energy of the M_4 edge. There is a clear two component line shape similar to those reported in the literature in this and other materials [11]. The width of the sharp component of the specular q scan corresponds with approximately 450 ordered layers; see inset of Fig. 4(a). Simulation of the scan of the incident photon energy at the Bragg position is shown by the solid line in Fig. 4(b). The deduced number of layers agrees well with that from the specular q scan. The experimental energy HWHM is 3.8 eV. The energy cut in the broad part of the q response, at (0 0 2.92), is given in Fig. 4(c). It is clear that the response is *narrower* in energy (HWHM ~ 2.5 eV) corresponding with only a few diffracting layers *located near the sample surface*. The fitted line is calculated with six magnetic layers counting down from the surface; simulations show that the uppermost of these layers cannot be located more than ten lattice spacings below the sample surface. This supports an independent result in UP, arrived at through a combination of xres and neutron scattering, both elastic and inelastic, where it was found that the broad component observed in xres was not due to thermodynamic fluctua-

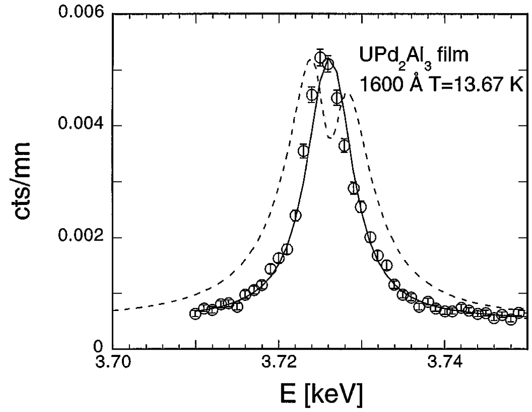

FIG. 3. Energy profile of the (0 0 0.5) reflection measured from a 1600 Å film of UPd_2Al_3 at 13.67 K, in the vicinity of T_N. The solid line is a calculation assuming that the scattering volume comprises just the top 600 (±50) Å, whereas the dashed line is the expected profile if this scattering volume were placed at the base of the film.

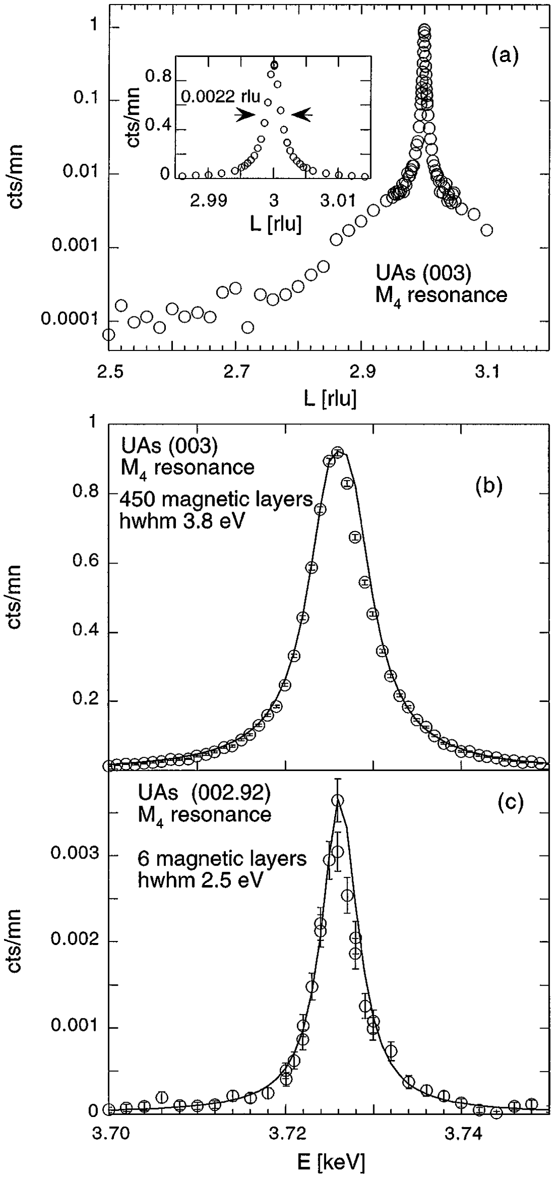

FIG. 4. Data from a thick crystal of UAs. (a) Wave vector scan, with photon energy tuned to the uranium M_4 absorption edge at 3.728 keV, about the (0 0 3) magnetic reflection. The inset shows detail of the sharp component on a linear vertical scale. (b) Energy scan of the sharp component, i.e., at the position $L = 3$ reciprocal lattice units (rlu) in Fig. 3(a). The line is a calculation with 450 magnetic layers (in agreement with the width of the L scan), i.e., reflection coming from the bulk of the crystal. Energy HWHM = 3.8 eV. (c) Energy scan of the broad component, i.e., at the position $L = 2.92$ rlu in Fig. 3(a). The line is a fit to a model with only six magnetic layers (~35 Å) down from the surface contributing to the intensity. Energy HWHM = 2.5 eV.

tions [11–14]. These observations, while not invalidating the work with xres on the two length scale problems [11], do motivate a careful reexamination of the experimental conditions and the possible role of the probe coherence volume.

In conclusion, we have introduced the idea that the probe coherence volume plays an increasingly important role in the interpretation of diffraction data. Such effects can be anticipated to arise more frequently as new generation experiments, both neutron and x ray, take data at increasingly better resolution. As the degree of partial coherence of the incident beam becomes significant, for example, in the vicinity of a phase transition, a reexamination of assumptions conventionally used to interpret diffraction profiles will be required. Indeed, unusual wave vector profiles at fixed incident energy, not discussed here, may also occur which likewise call into question the use of deconvolution at the level of intensities [6]. Since the latter assumption is conventionally used in treating data obtained through the anomalous scattering cross section (exploiting the element specificity of an absorption edge) in fields as varied as biology and materials science, our observations are of general interest for those using beams from the new synchrotrons, which inevitably exhibit a certain degree of coherence. By two examples, it has been shown that the energy dependence of scattering at a resonant absorption edge can give the spatial localization, *below the sample surface*, of the scattering centers. This previously inaccessible information has proved important in modeling the microscopic nature of the phase transition.

Support given to N.B. and S.L. in the frame of the EC funded training program (Human Capability and Mobility) is acknowledged. N.B. also acknowledges partial support from the Institute of Transuranium Elements in Karlruhe and the continuous support of the ILL, Grenoble, France.

[1] L. van Hove, Phys. Rev. **95**, 249 (1954).
[2] W. Marshall and S.W. Lovesey, *Theory of Thermal Neutron Scattering* (Oxford University Press, Oxford, 1971); M. Blume, J. Appl. Phys. **57**, 3615 (1985).
[3] M. Born and E. Wolf, *Principles of Optics* (Pergamon Press, New York, 1993), 6th ed.
[4] S.K. Sinha *et al.*, Phys. Rev. B **57**, 2740 (1998).
[5] M. Sutton *et al.*, Nature (London) **352**, 608 (1991); S. Brauer *et al.*, Phys. Rev. Lett. **74**, 2010 (1995); G. Grübel and D.L. Abernathy, Proc. SPIE Int. Soc. Opt. Eng. **3154**, 103 (1997).
[6] N. Bernhoeft, Acta Crystallogr. (to be published).
[7] J.O. Cross *et al.*, Phys. Rev. B (to be published).
[8] B.E. Warren, *X-ray Diffraction* (Addison-Wesley, Reading, MA, 1969).
[9] M. Huth *et al.*, Solid State Commun. **87**, 1133 (1993); M. Huth *et al.*, Physica (Amsterdam) **199–200B**, 116 (1994).
[10] H. Kita *et al.*, J. Phys. Soc. Jpn. **63**, 726 (1994); B. Gaulin *et al.*, Phys. Rev. Lett. **73**, 890 (1994).
[11] R.A. Cowley, Phys. Scr. **T66**, 24–30 (1996), and references therein.
[12] N. Bernhoeft *et al.*, J. Magn. Magn. Mater. **140-144**, 1421–1422 (1995).
[13] A. Stunault *et al.*, Phys. Rev. B **55**, 423–438 (1997).
[14] D. Wermeille *et al.*, Phys. Rev. B **58**, 3180 (1998).